Dendritic Spine Instability in a Mouse Model of CDKL5 Disorder Is Rescued by Insulin-like Growth Factor 1

Dendritic Spine Instability in a Mouse Model of CDKL5 Disorder Is Rescued by Insulin-Like Growth Factor 1

Supplemental Information

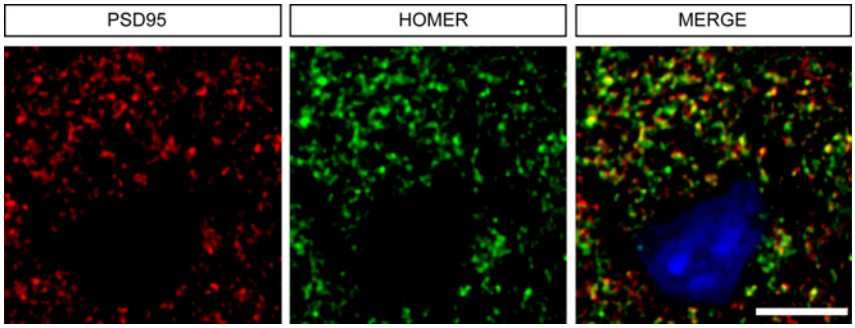

Figure S1. Representative images of cortical section immunolabelled with PSD-95 (red), Homer (green) and Nissl staining (blue). Merge shows the complete synaptic colocalization between PSD-95 and Homer puncta (yellow). Scale bar 5 µm.

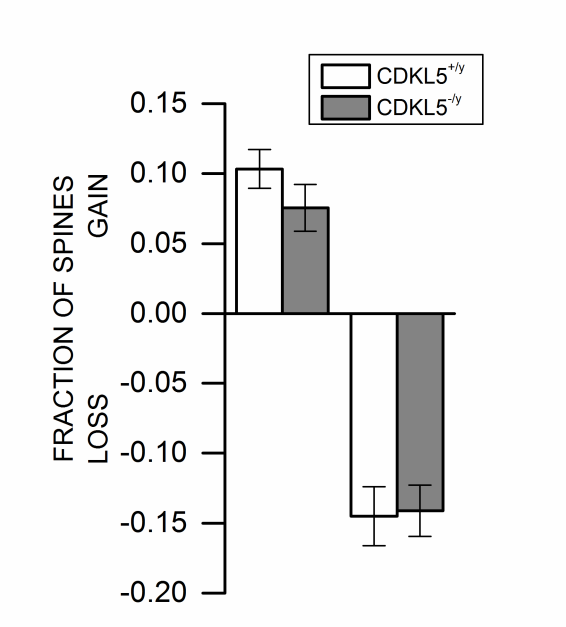

Figure S2. Short-term turnover of dendritic spines is not affected in adult CDKL5$^{-/y}$ mice. The plot indicates the fraction of spines that are formed (gain) or lost (loss) between 4 days of imaging from P50 until P54.

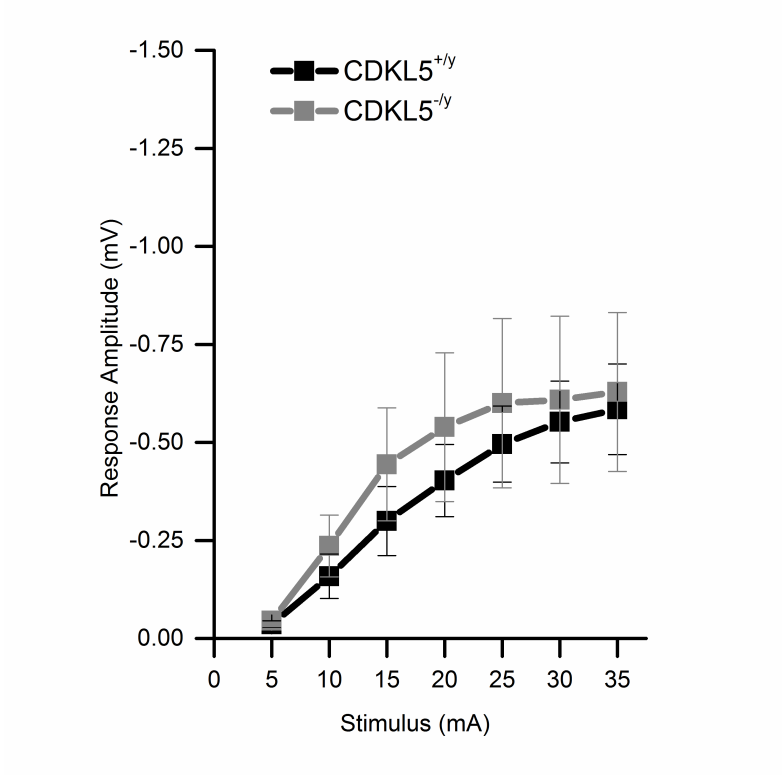

Figure S3. Input/output curves of EPSPs in CDKL5$^{-/y}$ and CDKL5$^{+/y}$ mice.

Supplemental Methods & Materials

Thinned Skull Surgery in Younger Mice at P27

The skull was exposed with a midline scalp incision and a region (~1 mm in diameter) overlying the somatosensory cortex based on stereotaxic coordinates A/P (-1) and L (1.58) from bregma. A high-speed drill was used carefully to reduce the skull thickness by ~50%. Skull thinning was then completed by scraping the cranial surface with a micro-surgical blade. To avoid damaging (evidenced post-hoc by dendritic blebbing, for example) the underlying cortex by friction-induced heat, a cool sterile solution was added to the skull periodically, and drilling was intermittent to permit heat dissipation (1). Optimal image quality was ensured by reducing skull thickness to a very thin layer (~30–50 µm). The animal was imaged immediately after surgery at P27 and the following day.

Chronic Window Surgery

The implant of chronic window was performed at P30, however the mouse was left to recover for 20 days and the imaging started at P50 (2,3) . The surgery began with the implantation of a metallic bar headpost. Firstly the scalp hair was gently trimmed, the skin disinfected with povidone-iodine and 70% ethanol solutions, and a central incision was performed. The skull was then scrubbed gently to remove the periosteum and dried. A layer of cyanoacrylate-based glue was then applied and a custom metallic bar headpost was cemented to the skull with dental acrylic. The headpost served to immobilize the mouse's head during imaging, while leaving an opening on the somatosensory barrel cortex. The second step was the creation of a craniotomy with an electric drill running at low speeds. Care was taken to minimize injury to the dura while drilling and removing skull fragments. Debris and blood from the dura were cleaned via frequent washes of sterile solution. A 5 mm sterile glass coverslip was placed into the craniotomy, and sealed with a small amount of cyanoacrylate glue between the edge of

the coverslip and the skull. As a final step dental acrylic was applied throughout the skull surface anchoring the window and sealing it from pathogens. After the surgery the animal was monitored on a heated blanket until it recovered from anaesthesia.

Data Analysis

ImageJ software was used to analyze image stacks of dendritic segment. The same dendritic branch was identified from three-dimensional stacks taken from different time points having good image quality. Spines were classified as filopodia (protrusions without an enlargement of the tip), thin (protrusions with a head smaller than spine length), stubby (large head spines without a neck), or mushroom (large head spines with a neck). All clear protrusions, regardless of their shape (stubby, mushroom, thin spines), emanating laterally from the dendrite were measured.

For each imaging session, the following parameters were calculated: spine density (number of spines for dendritic length), fraction of gained and lost spines (Gain and Loss) and survival as previously described (4). The time-dependent survival function was calculated as $SF(t)=N(t)/N_0$, where N_0 is the number of spines at $t=0$, and $N(t)$ is the number of spines of the original set surviving after time t. Similarly, gain and loss are expressed as [Gain = N_{gained}/N_{total} or Loss= N_{lost}/N_{total}] .

New persistent spines were defined as spines that were not present at the first time point (P50), but were gained at P54 and were present until P65.

Spine dimensions were performed with a custom made software (MATLAB program) that allowed visualization of the spine in the best possible plane. Spine length was measured from the dendritic shaft until the furthest point which contained a fluorescence. Spine head was measured along the dimension that maximized head width.

LTP Recordings

Brains were rapidly removed and immersed in ice-cold cutting solution. Coronal slices (350 μm thick) from 75-80 days old CDKL5$^{+/y}$ and CDKL5$^{-/y}$ mice, were obtained using a Leica VT1000S vibrating blade microtome. Slices were allowed to equilibrate in cutting solution at room temperature for at least 1 h before being transferred to a recording interface chamber and perfused at a rate of 4 ml/min with 30°C oxygenated recording solution. Cutting solution contained 132.8 mM NaCl, 3.1 mM KCl, 1 mM $CaCl_2$, 2 mM $MgCl_2$, 1 mM K_2HPO_4, 4 mM $NaHCO_3$, 5 mM D-glucose, 0.01 mM glycine, 1 mM ascorbic acid, 0.5 mM myo-inositol, 2 mM pyruvate, 10 mM HEPES, adjusted to pH 7.35. Recording solution had the same composition as cutting solution, except 2 mM $CaCl_2$, 1 mM $MgCl_2$.

Electrical stimulation in layer 2/3 of the somatosensory cortex (100 μs duration) was delivered with a bipolar concentric stimulating electrode (FHC, St. Bowdoinham, ME). Field excitatory post-synaptic potentials (fEPSPs) of the horizontal connections in layer 2/3 were recorded by a micropipette (1–3 MΩ) filled with the recording solution. We first measured the fEPSP amplitudes evoked by progressive increases in the stimulation intensity (input/output curves, I/O curves). Then, baseline responses were obtained every 60 s with a stimulation intensity that yielded a half-maximal response. After achievement of a 20 min stable baseline, long-term potentiation (LTP) was induced by a single TBS (4 trains of 10 bursts, delivered at 5 Hz, inter-train interval: 15 s; burst composition: 4 stimuli at 100 Hz of 1 ms duration) through the stimulating electrode. Field recordings were filtered and digitized with an A/D board (National Instruments) driven by a custom acquisition software. LTP graphs are expressed as a percentage of the averaged baseline collected before LTP induction. We evaluated fEPSP potentiation for each group by comparing the last 20 min post-TBS to baseline.

Patch-Clamp Recordings

CDKL5$^{-/y}$ and CDKL5$^{+/y}$ mice (27 days old) were anesthetized by inhalation of isoflurane and decapitated. Brains were rapidly removed and submerged in cold and bubbled cutting artificial cerebrospinal fluid (ACSF). The cutting ACSF contained 126 mM NaCl, 3 mM KCl, 7 mM MgSO4, 1 mM NaHPO4, 5 mM NaHCO3, 10 mM HEPES, 0.5 mM CaCl2, 8 mM glucose, 3 mM sodium pyruvate, 0.45 mM ascorbic acid, 2.4 mM myo-Inositol, pH adjusted to 7.4 with NaOH. Sagittal sections (300 µm thick) containing primary somatosensory cortex (S1) were cut in cold ACSF by using a Leica VT1000S slicer. Slices were incubated in recording ACSF at 37°C for 20–25 min immediately after slicing and subsequently at room temperature. The recording ACSF contained 126 mM NaCl, 3 mM KCl, 2 mM MgSO4, 1 mM NaHPO4, 5 mM NaHCO3, 10 mM HEPES, 2 mM CaCl2, and 20 mM glucose, pH 7.4. The experiment started at least 1 hour after the beginning of room temperature storing. mEPSC recordings were performed holding the cells at -70 mV, in 32°C bubbled ACSF perfused at 2.5 ml/min, with 1 µM tetrodotoxin (TTX), 20 µM bicuculline, and 50 µM APV. The pipette solution contained 120 mM potassium gluconate, 10 mM KCL, 10 mM Hepes, 5 mM EGTA, 4 mM MgATP, 0.3 mM NaGTP, and 5 mM sodium phosphocreatine, pH adjusted to 7.3 with KOH. Somatic whole-cell recordings were obtained from visually identified GFP fluorescent pyramidal cells in layer V of S1 cortex. Cell identity was confirmed by morphological characteristics and firing rate. Glass pipette electrodes (2 to 4 MΩ resistance) were pulled from borosilicate capillaries (World Precision Instruments) by using a Sutter P97 Flame Brown Puller (Sutter Instruments). Data were acquired by using a Multiclamp 700A computer controlled amplifier (Molecular Devices) and signals were digitized by means of DigiData 1322A (Molecular Devices), low-pass filtered at 2 kHz. Data acquisition and analysis was performed by using Clampex 8.2 and Clampfit 10.3 (Molecular Devices).

Synaptosomal Preparation

CDKL5$^{+/y}$ and CDKL5$^{-/y}$ mice (27-28 days old) were killed by decapitation, somatosensory cortex was rapidly removed and tissue was weighted and primarily processed as follows (5,6). The tissues were homogenized at 4°C in lysis buffer composed by 0.32 M sucrose, and HEPES 1X at pH 7.4, using a glass Teflon tissue grinder. The homogenates were centrifuged (15 min; 1400 x *g*) to obtain a supernatant S1 and the nuclear fraction P1. From supernatant S1, by centrifugation (15 min; 14,000 x *g*), we obtained the crude synaptosomal fraction P2. The P2 fraction was then washed with 200 µl of lysis buffer and underwent further spin (20 min; 3700 x g). The pellet obtained was the pure synaptosomal fraction that was resuspended in 10 µl of PARIS (Life Technologies, Temecula CA USA) and stored at -80°C.

Western Blot

Protein concentration of the synaptosomal fraction was determined with the Bio-Rad protein assay kit. Total lysates were boiled in SDS sample buffer, separated by SDS–PAGE and blotted to nitrocellulose membrane (Bio-Rad). Filters were blocked in Blocking Odyssey Buffer (Licor) and incubated with primary antibodies for 16 h at 4°C following the instruction of Odyssey System (Licor). The following primary antibodies were used: PSD-95 (anti-mouse 1:500, Abcam), beta-actin (Anti-mouse 1:3000, Sigma) and S6 total and S6 240-244 (1:1000, Cell Signaling). After washing three times with PBS and Blocking Odyssey Buffer (Licor) 1:1, filters were incubated with secondary antibodies IRDye® 680LT/800CW Goat (Polyclonal) anti-mouse IgG; 1:20000 (Licor) for 2 h at room temperature. Detection was performed by Odyssey System CLX. For quantitative measurements signal intensity was assessed with ImageJ (NIH) software.

Elisa Assay

We used the Quantikine mouse/rat IGF-1 Immunoassay ELISA kit (R&D Systems) according to manufacturer's instructions to assess IGF1 expression in cortex. Absorbance values were read at 450 nm in a plate reader (iMark Bio-Rad). P27 and P90 cortex were homogenized with 1% Triton X-100 and PBS with a phosphatase and protease inhibitor cocktail (Roche Diagnostics) and centrifuged at 14,000 *g* for 5 min (7). The supernatant was stored at –80°C until use.

Immunofluorescence and Punctate Staining Analysis

For detection of PSD-95, mice were deeply anesthetized with chloral hydrate and decapitated. The brains were excised and manually cut in coronal slabs that were fixed by immersion in ice-cold paraformaldehyde (4% in 0.1 M phosphate buffer, PB, pH 7.4) for 30 min (8). After fixation, tissue slabs were rinsed in PB, cryoprotected by immersion in ascending sucrose solutions (10, 20 and 30%), cut in 20-µm sections with a cryostat, mounted on gelatin-coated slides and stored at −20°C until immunolabeling was performed. Following a blocking step in normal donkey serum (3% in PBS with 0.5% Triton X-100), the sections were incubated overnight with anti-PSD-95 antibody (mAb; 1:500; Neuromab; CA, USA) at 4°C and subsequently with an anti-mouse secondary antibody conjugated to the cyanine-derived Cy3 (Jackson Immunoresearch, West Grove, PA) for 1 hour at room temperature. In double-labeling experiments, sections were simultaneously incubated with anti-PSD-95 and anti-panHomer (rabbit; 1:500; Synaptic System, Germany) antibodies followed by anti-mouse and anti-rabbit secondary antibodies conjugated to the cyanine-derived Cy3 and Alexa-633 respectively (Jackson Immunoresearch, West Grove, PA). Double-labeled sections were counterstained with a fluorescent Nissl staining solution (1:400; Life Technologies, USA).

The sections were rinsed again and cover slipped with Dako fluorescence mounting medium (Dako Italia, Italy).

Quantitative analyses of PSD-95-immunoreactive puncta were performed on 5 mice per genotype at P28 and on 6 mice per genotype at P56. Synaptic puncta were analyzed on 5 serial optical sections (0.5 µm Z-step size) that were acquired from layers 2-3 and 5 of the primary somatosensory cortex (S1) with a laser scanning confocal microscope (LSM5 Pascal; Zeiss, DE) using a 100× objective (1.4 numerical aperture) and the pinhole set at 1 Airy unit. The number of PSD-95-positive puncta was determined by manually counting postsynaptic clusters in the neuropil using the Imaris Software (Bitplane, Zurich, CH) and expressed as puncta/100 μm^2. The percentage of immunocolocalization between PSD-95 and Homer-positive puncta was quantified by manually counting the number of overlapping double-positive puncta obtained building the "Colocalization channel" in Imaris Software in automatically thresholded images.

Statistics and Data Collection

Data were collected and analyzed by investigators blind to the genetic and treatment status of the animal. Only animals with an opaque cranial window were discarded. Sample size was estimated by power analysis using data present in the literature on spine alteration in mouse models of neurodevelopmental disorders and the effect of IGF-1 on synaptic morphological and molecular organization. For the IGF-1 treatment animals were randomly assigned to the various experimental groups caring that littermates were divided in the different experimental groups. To analyze data we used the paired *t*-test (to compare two repeated measures on the same subjects) and the *t*-test (to compare between different subjects). ANOVA was used to compare many groups, and binary data statistics (χ^2 test) to compare abundance in different classes. $P = 0.05$ was assumed as significance level. Statistical analysis was performed using

the Sigma Stat (Systat, USA) software. Data are expressed as mean ± standard error of mean (SEM). Asterisks in figures report p-values (*$p < 0.05$, **$p < 0.01$, ***$p < 0.001$).

Supplemental References

1. Yang G, Pan F, Parkhurst CN, Grutzendler J, Gan WB (2010): Thinned-skull cranial window technique for long-term imaging of the cortex in live mice. *Nat Protoc*. 5:201-208.

2. Jiang M, Ash RT, Baker SA, Suter B, Ferguson A, Park J, *et al.* (2013): Dendritic arborization and spine dynamics are abnormal in the mouse model of MECP2 duplication syndrome. *J Neurosci*. 33:19518-19533.

3. Holtmaat A, Bonhoeffer T, Chow DK, Chuckowree J, De Paola V, Hofer SB, *et al.* (2009): Long-term, high-resolution imaging in the mouse neocortex through a chronic cranial window. *Nat Protoc*. 4:1128-1144.

4. Holtmaat AJ, Trachtenberg JT, Wilbrecht L, Shepherd GM, Zhang X, Knott GW, *et al.* (2005): Transient and persistent dendritic spines in the neocortex in vivo. *Neuron*. 45:279-291.

5. Huttner WB, Schiebler W, Greengard P, De Camilli P (1983): Synapsin I (protein I), a nerve terminal-specific phosphoprotein. III. Its association with synaptic vesicles studied in a highly purified synaptic vesicle preparation. *J Cell Biol*. 96:1374-1388.

6. Pavlowsky A, Gianfelice A, Pallotto M, Zanchi A, Vara H, Khelfaoui M, *et al.* (2010): A postsynaptic signaling pathway that may account for the cognitive defect due to IL1RAPL1 mutation. *Curr Biol*. 20:103-115.

7. Ueno M, Fujita Y, Tanaka T, Nakamura Y, Kikuta J, Ishii M, *et al.* (2013): Layer V cortical neurons require microglial support for survival during postnatal development. *Nat Neurosci*. 16:543-551.

8. Giustetto M, Kirsch J, Fritschy JM, Cantino D, Sassoe-Pognetto M (1998): Localization of the clustering protein gephyrin at GABAergic synapses in the main olfactory bulb of the rat. *J Comp Neurol*. 395:231-244.